Oscillatory superconducting transition temperature in superconductor/antiferromagnet heterostructures

G. A. Bobkov,[1] V. M. Gordeeva,[1] A. M. Bobkov,[1] and I. V. Bobkova[1,2]
[1]*Moscow Institute of Physics and Technology, Dolgoprudny, 141700 Moscow region, Russia*
[2]*National Research University Higher School of Economics, 101000 Moscow, Russia*

(Received 31 July 2023; revised 20 October 2023; accepted 23 October 2023; published 13 November 2023)

One of the most famous proximity effects at ferromagnet/superconductor (FM/SC) interfaces is partial conversion of singlet superconductivity to triplet pairing correlations. Due to the presence of macroscopic exchange field in the ferromagnet the Cooper pairs penetrating into the ferromagnet from the superconductor acquire a finite momentum there. The finite-momentum pairing manifests itself, in particular, as a nonmonotonic dependence of the critical temperature of the bilayer on the thickness of the FM layer. Here we predict that despite the absence of the macroscopic exchange field the critical temperature of the antiferromagnet/superconductor (AFM/SC) bilayers also exhibit nonmonotonic (oscillating) dependence on the AFM layer thickness. It is a manifestation of the proximity-induced Néel-type triplet correlations, which acquire finite total pair momentum and oscillate in the AFM layer due to the Umklapp electron-scattering processes at the AFM/SC interface. Our prediction can provide a possible explanation for a number of recently published experimental observations of the critical temperature of AFM/SC bilayers.

DOI: 10.1103/PhysRevB.108.184509

I. INTRODUCTION

Materials with magnetic ordering and superconductors both have prominent roles in condensed-matter physics due to their fundamental and technological interest. In particular, magnets are key elements of various spintronic applications and superconductors manifest perfect diamagnetism and dissipationless transport. Such physics is interesting in itself and is implemented in these materials separately. However, when we combine these materials, new physics related to the nanoscale interface region between them can occur. In general it is called proximity effects.

One of the most famous proximity effects at ferromagnet/superconductor (FM/SC) interfaces is partial conversion of singlet superconductivity to triplet pairing correlations [1,2]. The triplet pairs can sustain dissipationless spin currents and, consequently, are cornerstone elements in superconducting spintronics [3,4]. The triplet pairs arise at the expense of singlet correlations and thus suppress singlet superconductivity. One of the important properties of the triplet pairs generated at FM/SC interfaces is the finite momentum of the pair [5,6], which allows them to be called a mesoscopic analog of the inhomogeneous Fulde-Ferrel-Larkin-Ovchinnikov (FFLO) superconducting state [7,8]. The finite momentum which the Cooper pair acquires in the exchange field of the ferromagnet makes the pairing wave function oscillate. The resulting phase change across the ferromagnetic layer is responsible for the π-junction effects [1,5,9–13], which are widely used now in the superconducting electronics [14–16]. The interference of the incident and reflected oscillating wave functions determines the oscillatory phenomena of the critical temperature T_c versus the FM layer thickness in FM/SC bilayers and multilayers, which have been widely studied both theoretically [17–22] and experimentally [23–27].

At present, there is another direction of superconducting spintronics, which is based on superconductor/antiferromagnet (AFM/SC) heterostructures. It is often called antiferromagnetic superconducting spintronics and looks very promising due to several advantages brought by antiferromagnets, such as negligible stray fields and intrinsic high-frequency dynamics [28–30], and also due to unique features of the proximity effect at AFM/SC interfaces [31–43], in particular, the possibility to control the anisotropy of the Néel vector by superconductivity [44] and AFM/SC/AFM spin valves [45].

Analogously to FM/SC interfaces the singlet-triplet conversion was also reported even at fully compensated AFM/SC interfaces [36], but the amplitude of the corresponding oscillations flips its sign between the nearest-neighbor sites of the lattice in the superconductor in the same way as the Néel magnetic order does. For this reason the corresponding triplet correlations were called Néel triplets. The influence of the Néel triplets on superconducting critical temperature has already been investigated in thin-film AFM/SC heterostructures [36,37], which can be viewed as homogeneous superconductors in uniform Néel exchange field. However, their behavior in metallic antiferromagnets of finite width, proximitized by a superconductor, has not been studied yet. In this work we fill this gap. Naively, one does not expect that a Cooper pair penetrating into the antiferromagnet from the superconductor possesses a finite total momentum because the average value of the exchange field in the antiferromagnet is zero, the quasiparticles spectrum is spin-degenerate and, therefore, spin-up and spin-down electrons, forming the pair, should have opposite momenta with equal absolute values $\boldsymbol{p}_\uparrow = -\boldsymbol{p}_\downarrow$. In its turn, that means zero total momentum of the pair and, as a result, absence of the oscillations of the pair amplitude. Consequently, one does not expect oscillating behavior of

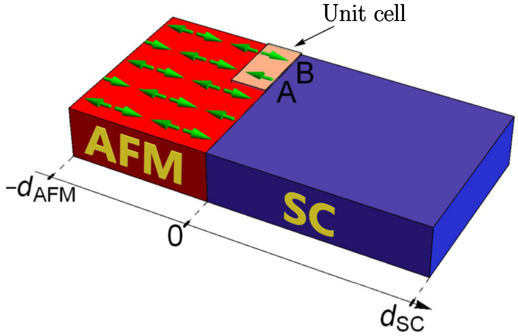

FIG. 1. AFM/SC bilayer. Staggered magnetization of the AFM layer is schematically depicted by arrows. The unit cell containing two sites belonging to A and B sublattices is also shown.

the critical temperature of AFM/SC bilayers in dependence on the thickness of the antiferromagnetic layer. Indeed, in the regime, when the Néel triplets can be disregarded, this dependence has been calculated and no oscillations were reported [43].

However, there are a number of experimental works, where the critical temperature of AFM/SC bilayers with metallic antiferromagnets has been measured as a function of the AFM thickness and the oscillating behavior was observed [46–48]. Here we demonstrate theoretically that taking into account the Néel triplet correlations at AFM/SC interfaces results in the oscillating dependence of the critical temperature on the AFM thickness and unveil physical mechanisms of the effect. Thus, oscillations of the critical temperature of AFM/SC bilayers can be viewed as a signature of the presence of Néel-type triplet correlations in the heterostructure.

The paper is organized as follows: In Sec. II we describe the considered model and the formalism used for calculations. In Sec. III our results are presented: Sec. III A is devoted to discussion of spatial oscillations of the triplet pair correlations, induced in the AFM layer by proximity to the superconductor, and in Sec. III B we show the results for the critical temperature and discuss how it depends on the parameters of the AFM/SC heterostructure. Our conclusions are presented in Sec. IV. In the Appendix we provide some technical details of the calculation of the Green's function.

II. MODEL AND METHOD

We consider an AFM/SC bilayer system, presented in Fig. 1. It is composed of a conventional s-wave singlet superconductor with thickness $d_{\rm SC}$ and a metallic antiferromagnet with thickness $d_{\rm AFM}$. The system is described by the following tight-binding Hamiltonian in the two-sublattice representation:

$$\hat{H} = -t \sum_{\langle \boldsymbol{i}\boldsymbol{j}\nu\bar{\nu}\rangle,\sigma} \hat{\psi}^{\nu\dagger}_{\boldsymbol{i}\sigma}\hat{\psi}^{\bar{\nu}}_{\boldsymbol{j}\sigma} + \sum_{\boldsymbol{i},\nu}\left(\Delta_{\boldsymbol{i}}^{\nu}\hat{\psi}^{\nu\dagger}_{\boldsymbol{i}\uparrow}\hat{\psi}^{\nu\dagger}_{\boldsymbol{i}\downarrow} + \text{H.c.}\right) - \mu\sum_{\boldsymbol{i}\nu,\sigma}\hat{n}^{\nu}_{\boldsymbol{i}\sigma} + \sum_{\boldsymbol{i}\nu,\alpha\beta}\hat{\psi}^{\nu\dagger}_{\boldsymbol{i}\alpha}\left(\boldsymbol{h}^{\nu}_{\boldsymbol{i}}\boldsymbol{\sigma}\right)_{\alpha\beta}\hat{\psi}^{\nu}_{\boldsymbol{i}\beta}. \quad (1)$$

The unit cell with two sites A and B is introduced as shown in Fig. 1. In the framework of this two-sublattice approach the unit cells as a whole are marked by radius-vector $\boldsymbol{i}$. $\nu = A, B$ is the sublattice index, $\bar{\nu} = A$ (B) if $\nu = B$ (A) means that the corresponding quantity belongs to the opposite sublattice. $\langle \boldsymbol{i}\boldsymbol{j}\nu\bar{\nu}\rangle$ means summation over the nearest neighbors, $\hat{\psi}^{\nu\dagger}_{\boldsymbol{i}\sigma}$ $(\hat{\psi}^{\nu}_{\boldsymbol{i}\sigma})$ is the creation (annihilation) operator for an electron with spin σ at the sublattice ν of the unit cell $\boldsymbol{i}$. t parametrizes the hopping between adjacent sites, μ is the electron chemical potential counted from the middle of the conduction band (that is $\mu = 0$ corresponds to half filling), and $\hat{n}^{\nu}_{\boldsymbol{i}\sigma} = \hat{\psi}^{\nu\dagger}_{\boldsymbol{i}\sigma}\hat{\psi}^{\nu}_{\boldsymbol{i}\sigma}$ is the particle number operator at the site belonging to sublattice ν in unit cell $\boldsymbol{i}$. For simplicity the hopping parameter is assumed to be equal in the regions occupied by the superconductor and by the antiferromagnet. At the same time, we take into account difference between chemical potentials in the SC and AFM regions $\mu_{\rm SC} \neq \mu_{\rm AFM}$. It is worth mentioning that, for the equilibrium problem under consideration, the filling levels of electronic states in the SC and AFM layers are the same. Different $\mu_{\rm SC}$ and $\mu_{\rm AFM}$ mean that conduction bands of the materials are shifted relative to each other. The staggered magnetism is described by $\boldsymbol{h}^{A(B)}_{\boldsymbol{i}} = +(-)\boldsymbol{h}_{\boldsymbol{i}}$, where $\boldsymbol{h}_{\boldsymbol{i}}$ is the local magnetic moment at site A of the unit cell with the radius vector $\boldsymbol{i}$ in the AFM. This allows us to consider $\boldsymbol{h}_{\boldsymbol{i}}$ as a slow function of the spatial coordinate. We consider the homogeneously ordered Néel state of the AFM here, such that $\boldsymbol{h}_{\boldsymbol{i}} = \boldsymbol{h}$ does not depend on the position $\boldsymbol{i}$ inside the antiferromagnet and has zero value in the superconductor. We assume that the AFM/SC interface is fully compensated, that is the interface exchange field is staggered with zero average value. $\Delta^{\nu}_{\boldsymbol{i}}$ accounts for on-site s-wave pairing and has nonzero value only in the superconductor. In case of conventional singlet pairing $\Delta^{A}_{\boldsymbol{i}} = \Delta^{B}_{\boldsymbol{i}} = \Delta_{\boldsymbol{i}}$.

The system, described by Hamiltonian (1), can be treated in the framework of the two-sublattice quasiclassical theory [36]. In this formalism all the characteristic spatial scales are large as compared with interatomic distance and, therefore, the discrete unit-cell index $\boldsymbol{i}$ can be changed by the continuous spatial variable $\boldsymbol{R}$. The system is described by the quasiclassical Green's function $\check{g}(\boldsymbol{R}, \boldsymbol{p}_{\rm F}, \omega_m)$, which is an 8×8 matrix in the direct product of spin, particle-hole and sublattice spaces and depends on the radius vector $\boldsymbol{R}$, direction of the electron momentum at the Fermi surface $\boldsymbol{p}_{\rm F}$, and fermionic Matsubara frequency $\omega_m = \pi T(2m+1)$. It obeys the following Eilenberger equation [36]:

$$[(i\omega_m\tau_z + \mu + \tau_z\check{\Delta}(\boldsymbol{R}) - \boldsymbol{h}(\boldsymbol{R})\boldsymbol{\sigma}\tau_z\rho_z)\rho_x, \check{g}(\boldsymbol{R}, \boldsymbol{p}_{\rm F}, \omega_m)] + i\boldsymbol{v}_{\rm F}\nabla\check{g}(\boldsymbol{R}, \boldsymbol{p}_{\rm F}, \omega_m) = 0, \quad (2)$$

where $\boldsymbol{v}_{\rm F}$ is the Fermi velocity for the trajectory $\boldsymbol{p}_{\rm F}$, and $\boldsymbol{\sigma} = (\sigma_x, \sigma_y, \sigma_z)^T$ is the vector of Pauli matrices in spin space. Analogously, τ_i and ρ_i are Pauli matrices in the particle-hole and sublattice spaces, respectively. As shown in Fig. 1, the AFM layer occupies the region $-d_{\rm AFM} < x < 0$, and the SC layer is at $0 < x < d_{\rm SC}$. We assume translational invariance along the AFM/SC interface, consequently the Green's function only depends on the x coordinate, normal to the interface. For brevity we define $|\boldsymbol{v}_{F,x}| = v$ and $\check{\Delta}(\boldsymbol{R}) = \Delta(\boldsymbol{R})\tau_x$. The quasiclassical Green's function for a given trajectory $\check{g}(x, \pm v) \equiv \check{g}^{\pm}(x)$ also obeys the normalization condition

$$[\check{g}^{\pm}(x)]^2 = 1 \quad (3)$$

and boundary conditions at the AFM/SC interface $x=0$ and at the impenetrable edges of the AFM ($x=-d_{\rm AFM}$) and SC ($x=d_{\rm SC}$) layers. Since we consider identical lattices in the AFM and SC layers and ($\mu_{\rm AFM}, \mu_{\rm SC}$) are assumed to be small with respect to t to be considered in the framework of the quasiclassical approximation, the interface barrier at $x=0$ is absent. In this case the boundary conditions at $x=0$ are reduced to continuity of the Green's functions, analogously to the case of superconductor/normal metal and superconductor/ferromagnet interfaces [49,50]:

$$\check{g}^{{\rm SC},\pm}(x=0)=\check{g}^{{\rm AFM},\pm}(x=0). \quad (4)$$

The boundary conditions at the impenetrable edges are reduced to the equality of the incident and reflected Green's functions [49]:

$$\check{g}^{{\rm SC},+}(x=d_{\rm SC})=\check{g}^{{\rm SC},-}(x=d_{\rm SC}),$$
$$\check{g}^{{\rm AFM},+}(x=-d_{\rm AFM})=\check{g}^{{\rm AFM},-}(x=-d_{\rm AFM}). \quad (5)$$

We assume $d_{\rm SC}$ to be much smaller than all the characteristic spatial scales of the anomalous Green's function in the superconductor. One of them is the superconducting coherence length $\xi_{\rm S}=v_{\rm F}/2\pi T_{c0}$ and the other one is the length of spatial oscillations of the triplet components of the anomalous Green's function, which will be discussed below. In this case the superconducting order parameter is approximately spatially constant inside the SC layer, $\Delta(\boldsymbol{R})=\Delta$.

For the problem under consideration the Néel vector of the AFM is spatially homogeneous. In this case the Green's function is diagonal in spin space and we work with its components in spin space $\check{g}_\sigma$, which are still 4×4 matrices in the direct product of particle-hole and sublattice spaces. $\sigma=\uparrow,\downarrow$ in the subscripts of all the quantities and $\sigma=\pm 1$ as a factor in the mathematical expressions for spin-up (-down) components, respectively. To find the critical temperature of the system we linearize the Eilenberger equation (2) with respect to Δ/T_c. In this approximation the Green's function takes the form:

$$\check{g}_\sigma=\begin{pmatrix}\check{g}_{\sigma,N} & \check{f}_\sigma \\ \check{\check{f}}_\sigma & \check{\check{g}}_{\sigma,N}\end{pmatrix}_\tau. \quad (6)$$

The diagonal components $\check{g}_{\sigma,N}$ and $\check{\check{g}}_{\sigma,N}$ are to be calculated in the normal state of the superconductor. The anomalous components $\check{f}_\sigma$ and $\check{\check{f}}_\sigma$ are of the first order with respect to Δ/T_c. The detailed calculations of the normal state Green's function $\check{g}_{\sigma,N}$ are presented in the Appendix. For the problem under consideration in the AFM layer it takes the form

$$\check{g}^{\rm AFM}_{\sigma,N}=A\left[\rho_x-\frac{i\sigma h}{\mu_{\rm AFM}+i\omega_m}\rho_y\right]+B\left[\frac{i\sigma h}{\Lambda}\rho_x+\frac{\mu_{\rm AFM}+i\omega_m}{\Lambda}\rho_y+\rho_z\right]e^{\beta x}+C\left[-\frac{i\sigma h}{\Lambda}\rho_x-\frac{\mu_{\rm AFM}+i\omega_m}{\Lambda}\rho_y+\rho_z\right]e^{-\beta x}, \quad (7)$$

where h is the absolute value of $\boldsymbol{h}$, $\Lambda=[h^2-(\mu_{\rm AFM}+i\omega_m)^2]^{1/2}$, $\beta=2\Lambda/v$, and the A, B, C coefficients are found from the boundary and normalization conditions. In the SC layer the Green's function takes the form

$$\check{g}^{\rm SC}_{\sigma,N}=G\rho_x+D[\rho_z+i\rho_y]e^{\lambda x}+E[\rho_z-i\rho_y]e^{-\lambda x}, \quad (8)$$

where $\lambda=2(\omega_m-i\mu_{\rm SC})/v$, and the G, D, E coefficients are found from the boundary and normalization conditions.

The hole component $\check{\check{g}}_N$ is obtained as follows:

$$\check{\check{g}}_{\sigma,N}(\omega_m,h,\mu)=-\check{g}_{\sigma,N}(-\omega_m,-h,\mu). \quad (9)$$

It is worth noting that, unlike FM/SC structures, for AFM/SC systems the normal-state Green's function $\check{g}_N$ is not identically equal to 1 and has a complicated structure with spatially constant and spatially oscillating components with strongly energy-dependent amplitudes. This originates from the energy dependence of the density of states near the Fermi surface because of the antiferromagnetic gap and possibility of Umklapp processes, see qualitative discussion of the nature of the oscillations below.

The anomalous components $\check{f}_\sigma$ and $\check{\check{f}}_\sigma$ are of the first order with respect to Δ/T_c. The resulting equation for the anomalous Green's function $\check{f}_\sigma$ takes the form:

$$\{(i\omega_m-h(x)\sigma\rho_z)\rho_x,\check{f}^\pm_\sigma\}+[\mu(x)\rho_x,\check{f}^\pm_\sigma]+\Delta(x)(\rho_x\check{\check{g}}^\pm_N-\check{g}^\pm_N\rho_x)\pm iv\frac{d}{dx}\check{f}^\pm_\sigma=0. \quad (10)$$

This equation can be rewritten in terms of the vector $\hat{f}^\pm_\sigma=(\check{f}^\pm_{\sigma,0},\check{f}^\pm_{\sigma,x},\check{f}^\pm_{\sigma,y},\check{f}^\pm_{\sigma,z})^T$, where the components of the vector correspond to the components of the expansion of $\check{f}^\pm_\sigma=\sum_i\check{f}^\pm_{\sigma,i}\rho_i$ over the Pauli matrices in the sublattice space:

$$\hat{F}_\sigma\hat{f}^\pm_\sigma+G^\pm_\sigma\pm iv\frac{d}{dx}\hat{f}^\pm_\sigma=0, \quad (11)$$

$$\hat{F}_\sigma=\begin{pmatrix}0 & 2i\omega_m & -2ih(x)\sigma & 0\\ 2i\omega_m & 0 & 0 & 0\\ -2ih(x)\sigma & 0 & 0 & -2i\mu(x)\\ 0 & 0 & +2i\mu(x) & 0\end{pmatrix}. \quad (12)$$

The same expansion $\check{g}^\pm_{\sigma,N}=\sum_i\check{g}^\pm_{\sigma,N,i}\rho_i$ is also introduced for the vector of the normal-state Green's function. Then

$$\hat{G}^\pm_\sigma=\begin{pmatrix}\Delta(x)\big(\check{\check{g}}^\pm_{\sigma,N,x}-\check{g}^\pm_{\sigma,N,x}\big)\\ 0\\ -i\Delta(x)\big(\check{\check{g}}^\pm_{\sigma,N,z}+\check{g}^\pm_{\sigma,N,z}\big)\\ i\Delta(x)\big(\check{\check{g}}^\pm_{\sigma,N,y}+\check{g}^\pm_{\sigma,N,y}\big)\end{pmatrix}. \quad (13)$$

We assume that the SC layer is thin with $d_{\rm SC}\ll\xi_{\rm S}$, then we can linearize Eq. (11) with respect to $x/\xi_{\rm S}$ and at the same time it is possible to consider the superconducting order parameter in the SC layer $\Delta(x)$ independent of coordinates $\Delta(x)\approx\Delta$. With this assumption, the solution of Eq. (11) takes the following form in the AFM and SC regions, respectively (the boundary conditions at $x=+d_{\rm SC},-d_{\rm AFM}$ are already taken into account):

$$\hat{f}^{\pm,{\rm AFM}}_\sigma=\sum_{\alpha=1}^4 K^\pm_{\alpha,\sigma}\hat{e}_\alpha e^{\mp i\kappa_\alpha(x+d_{\rm AFM})/v}, \quad (14)$$

$$\hat{f}^{\pm,{\rm SC}}_\sigma=\sum_{\alpha=1}^4 L^\pm_{\alpha,\sigma}\hat{s}_\alpha e^{\mp i\nu_\alpha(x-d_{\rm SC})/v}-\frac{(\hat{G}^\pm_\sigma\hat{s}_\alpha)\hat{s}_\alpha}{\nu_\alpha|s_\alpha|^2}, \quad (15)$$

where $\hat{e}_\alpha$, $\hat{s}_\alpha$ are eigenvectors of matrix $\hat{F}_\sigma^\pm$ in the AFM and SC regions, and κ_α, ν_α are eigenvalues of matrix $\hat{F}_\sigma^\pm$ in the AFM and SC regions, respectively. $K_{\alpha,\sigma}^\pm$, $L_{\alpha,\sigma}^\pm$ are unknown coefficients, which should be found from the boundary conditions at $x = 0$.

$$\hat{e}_{1,2} = \begin{pmatrix} \mu_{\text{AFM}} \\ \pm\sqrt{\mu_{\text{AFM}}^2 - h^2} \\ 0 \\ -h\sigma \end{pmatrix}, \quad \hat{e}_{3,4} = \begin{pmatrix} -h\sigma \\ 0 \\ \mp i\sqrt{\mu_{\text{AFM}}^2 - h^2} \\ +\mu_{\text{AFM}} \end{pmatrix}, \tag{16}$$

$$\hat{s}_{1,2} = \begin{pmatrix} 1 \\ \pm 1 \\ 0 \\ 0 \end{pmatrix}, \quad \hat{s}_{3,4} = \begin{pmatrix} 0 \\ 0 \\ \mp i \\ 1 \end{pmatrix}, \tag{17}$$

$$\kappa_{1,2} = \pm 2i\omega_m \frac{\mu_{\text{AFM}}}{\sqrt{\mu_{\text{AFM}}^2 - h^2}}, \quad \kappa_{3,4} = \pm 2\sqrt{\mu_{\text{AFM}}^2 - h^2}, \tag{18}$$

$$\nu_{1,2} = \pm 2i\omega_m, \quad \nu_{3,4} = \pm 2\mu_{\text{SC}}. \tag{19}$$

The exact expressions for $L_{\alpha,\sigma}$ and $K_{\alpha,\sigma}$ are rather lengthy and we do not write them here. However, for the case $\mu_{\text{SC}} = 0$, for which we present numerical results, the coefficients are written in the Appendix.

The critical temperature of the AFM/SC bilayer is calculated from the self-consistency equation

$$\Delta(x) = \int \frac{d\Omega}{4\pi} i\pi\lambda T_c \sum_{\omega_m} f_s(x), \tag{20}$$

where $\int d\Omega/4\pi$ means averaging over the Fermi surface, λ is coupling constant, and f_s is the amplitude of singlet correlations, which takes the form

$$f_s^\pm = \sum_\sigma \text{Tr}\left[\frac{\rho_x \check{f}_\sigma^\pm}{4}\right] = \sum_\sigma \left[\left(L_{1,\sigma}^\pm - L_{2,\sigma}^\pm\right) - \frac{\hat{G}_\sigma^\pm(\hat{s}_1 + \hat{s}_2)}{4i\omega_m}\right]. \tag{21}$$

At $d_{\text{SC}} \lesssim \xi_{\text{S}}$ the spatial dependence of the order parameter in the SC layer is weak, that is, $\Delta(x) \approx \Delta$. In this case $f_s(x)$ in Eq. (20) can be taken at $x = d_{\text{SC}}$ or we can take the average of the f_s over the SC layer. The result depends little on this.

III. RESULTS

A. Oscillations of the Néel triplet correlations in the antiferromagnet

Now we discuss the behavior of the singlet and Néel triplet correlations in the AFM layer. Figure 2 shows some typical examples of the spatial distribution of the singlet and triplet correlations inside the AFM layer. The anomalous Green's functions plotted in this figure are summed up over all positive Matsubara frequencies, that is

$$F_{s,t} = T \sum_{\omega_m > 0} f_{s,t}, \tag{22}$$

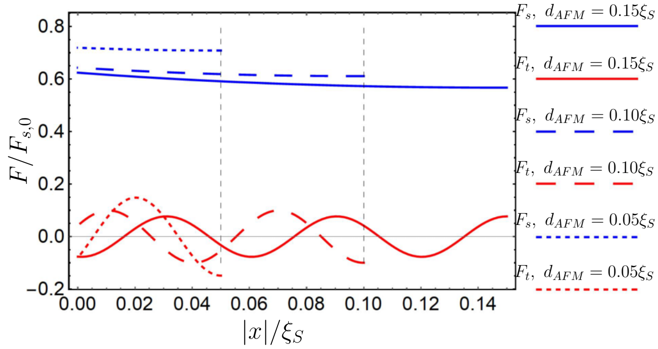

FIG. 2. Dependence of the triplet anomalous Green's function F_t(red) and the singlet anomalous Green's function F_s(blue) for the normal to the AFM/SC interface trajectory $v > 0$ on the distance from the interface inside the AFM layer. Different curves correspond to different thicknesses d_{AFM} of the AFM layer. Each of the curves ends at the distance corresponding to the impenetrable edge of the AFM layer. $d_{\text{SC}} = 0.5\xi_{\text{S}}$, $h = 0.6\mu_{\text{AFM}}$, $\mu_{\text{SC}} = 0$, $\mu_{\text{AFM}} = 420T_{c0}$, where T_{c0} is the critical temperature without the AFM layer. $F_{s,0}$ is the singlet anomalous Green's function in the absence of the AFM layer, see text for the details of the definitions of the Green's functions.

with

$$f_t = \frac{1}{4}\sum_\sigma \sigma \text{Tr}[\rho_y \check{f}_\sigma^\pm], \tag{23}$$

where $T \to T_c$. The anomalous Green's functions $F_{s,t}$ are normalized to the value of the singlet anomalous Green's function $F_{s,0}$ corresponding to the isolated SC layer without proximity to an antiferromagnet. The correlations presented in Fig. 2 correspond to the $v > 0$ trajectory normal to the AFM/SC interface.

From the results presented in Fig. 2 we conclude that the triplet correlations oscillate inside the antiferromagnet, while the singlet correlations just decay without oscillations. Now we discuss the physical explanation of the oscillating behavior. Let us consider an electron (p_{x1}, p_y) incoming to the AFM/SC interface from the AFM side (marked by 1 in Fig. 3). Due to proximity effect with the adjacent SC

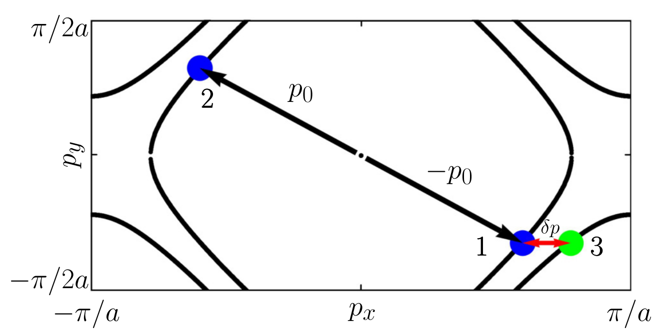

FIG. 3. BZ and Fermi surface (black curves) of the AFM layer. Zero-momentum Cooper pair between electrons 1 and 2 is schematically shown by black arrows. There is also Néel-type finite-momentum triplet pairing between electrons 2 and 3, which is produced from electron 1 due to the Umklapp reflection process from the AFM/SC interface, see text for details. The total momentum of the pair (2,3), δp, is shown by the red arrow.

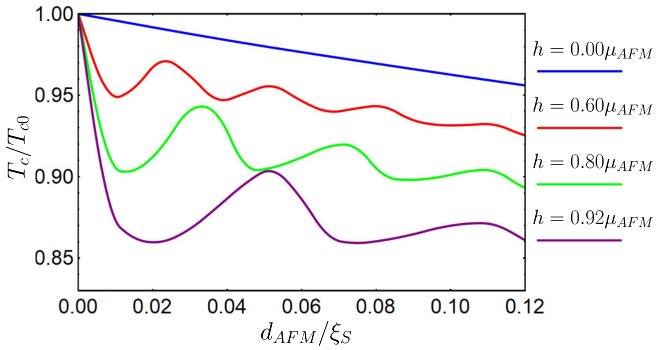

FIG. 4. Critical temperature of the AFM/SC bilayer as a function of the AFM layer thickness d_{AFM}. The critical temperature is normalized to its value without the AFM layer T_{c0}. $d_{\mathrm{SC}} = 1.5\xi_{\mathrm{S}}$, $\mu_{\mathrm{SC}} = 0$, $\mu_{\mathrm{AFM}} = 420T_{c0}$.

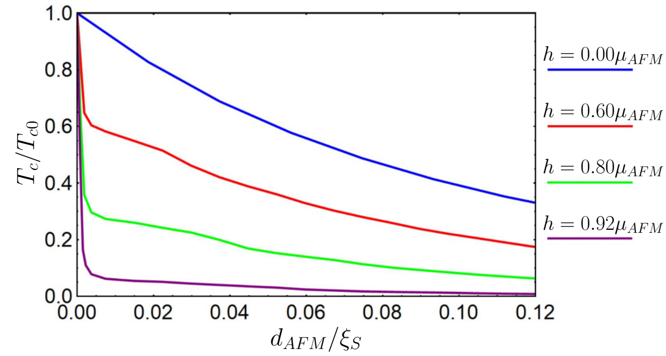

FIG. 6. The same as in Fig. 4 but for $d_{\mathrm{SC}} = 0.225\xi_{\mathrm{S}}$. The other parameters are the same.

layer it forms a singlet Cooper pair with another electron 2 corresponding to the momentum $(-p_{x1}, -p_y)$. For the plane interface the component of the electron momentum along the interface p_y is conserved. For the interface problem under consideration it is convenient to choose the Brillouin zone as shown in Fig. 3. Due to the doubling of the unit cell the Brillouin zone (BZ) is compressed twice in the interface direction. As a result, additional branches of the Fermi surface appear in the reduced BZ and the incoming electron 1 can be reflected as electron 3, corresponding to the same p_y (Umklapp process or the so-called Q reflection [33,34]). Due to the proximity-induced pairing correlations between electrons 1 and 2, the pairing is also established between electrons 2 and 3. It is the Néel-type triplet finite-momentum pairing and the total momentum of the pair (2,3) can be found as $\delta p = |p_{x3} - p_{x1}|$.

The normal-state electron dispersion in the reduced BZ takes the form $\varepsilon = -\mu_{\mathrm{AFM}} + [h^2 + 4t^2(\cos p_x a + \cos p_y a + \cos p_z a)^2]^{1/2}$. From this dispersion relation we obtain $\delta p = (\mu_{\mathrm{AFM}}^2 - h^2)^{1/2}/(ta \sin[p_x a])$. The last expression can be rewritten in terms of the electron Fermi velocity $v_{F,x} \equiv v = \partial\varepsilon/\partial p_x = 2ta \sin[p_x a]$ at $\mu_{\mathrm{AFM}} = h = 0$, which enters our quasiclassical theory, as $\delta p = 2(\mu_{\mathrm{AFM}}^2 - h^2)^{1/2}/v$. Please note that it is exactly the factor which determines oscillation behavior of the AFM anomalous Green's function in Eq. (14). Then the period of oscillations is

$$L_{\mathrm{osc}} = \frac{\pi v_{\mathrm{F}}}{\sqrt{\mu_{\mathrm{AFM}}^2 - h^2}}, \tag{24}$$

which is in agreement with the result of rigorous calculation of the anomalous Green's function, plotted in Fig. 2.

Unlike the case of SC/FM heterostructures, where both singlet and triplet correlations manifest oscillations with the same period inside the ferromagnet, here the singlet correlations do not oscillate. The reason is that, according to our qualitative consideration only Néel pairs can have finite momentum of such physical origin. However, in the considered case the Néel singlet pairs are not produced because of the absence of an appropriate scalar generator of the Néel type.

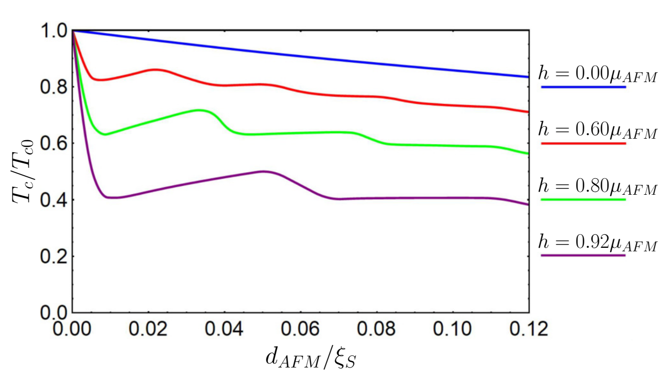

FIG. 5. The same as in Fig. 4 but for $d_{\mathrm{SC}} = 0.75\xi_{\mathrm{S}}$. The other parameters are the same.

B. Critical temperature of the AFM/SC bilayer

In AFM/SC bilayer systems with finite-width antiferromagnets the oscillating Néel triplet superconducting correlations discussed above can experience constructive or destructive interference due to the reflections from the impenetrable edge of the AFM layer. It leads to the oscillating dependence of the Néel triplet correlations amplitude as a function of d_{AFM}. In its turn, such a nonmonotonic dependence of the triplet amplitude results in the oscillating behavior of the critical temperature of the bilayer as a function of the AFM layer width d_{AFM}.

The results of the calculation of the critical temperature of the AFM/SC bilayer as a function of d_{AFM} are presented in Figs. 4–6. Different curves correspond to different exchange fields of the AFM layer. In all three figures we can see the superconductivity suppression accompanied by oscillations of the critical temperature. The amplitude of the oscillations grows with the value of the exchange field. Figure 4 demonstrates the results corresponding to rather thick superconductor layer. In this case the overall suppression of superconductivity is weak (pay attention to the scale of the vertical axis). It is obvious that in the limit of very thick SC layer all the manifestations of the proximity effect between SC and AFM in the critical temperature (that is, the suppression and the oscillations) vanish. In Fig. 5 the results for the moderate thickness of the SC layer are presented. The suppression of superconductivity as well as oscillations are more pronounced. In Fig. 6 the results for the thinnest SC

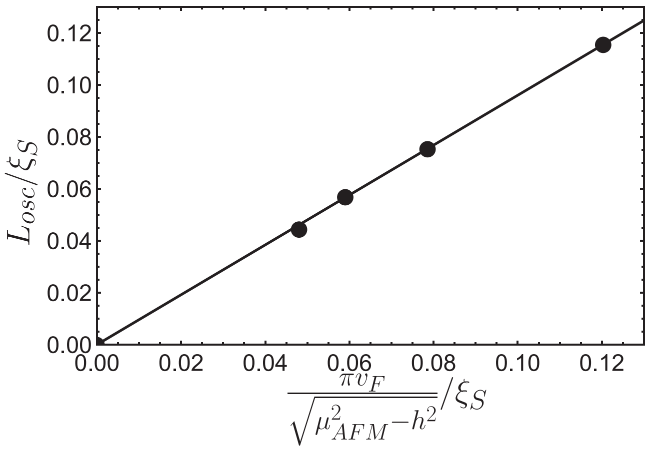

FIG. 7. Period of oscillations L_{osc} of the critical temperature for $h = 0.2\mu_{\rm AFM}$, $0.6\mu_{\rm AFM}$, $0.8\mu_{\rm AFM}$, and $0.92\mu_{\rm AFM}$ as a function of $\pi v_{\rm F}(\mu_{\rm AFM}^2 - h^2)^{-1/2}$.

layer are shown. The suppression of superconductivity is the strongest and for rather large values of the exchange field and thicknesses of the AFM layer the superconductivity can be completely suppressed. The amplitude of the oscillations is also weakly pronounced. It is due to the fact that the amplitude of the oscillating Néel triplets inside the AFM layer is greatly suppressed in this case because of the overall suppression of superconductivity. The period of the oscillations is described well by Eq. (24) regardless of the thickness of the superconductor. The oscillation period extracted from the results presented in Fig. 5 is shown by black points in Fig. 7, which are in excellent agreement with Eq. (24).

IV. CONCLUSIONS

In the present work an AFM/SC bilayer with metallic antiferromagnet is studied in the framework of the two-sublattice quasiclassical theory in terms of the Eilenberger equation for Green's functions. It is demonstrated that the proximity-induced Néel triplet correlations decay into the depth of the antiferromagnet is superimposed by oscillations. The period of the oscillations is determined by the finite momentum of the Néel triplet pairs in the antiferromagnet caused by the Umklapp scattering at the AFM/SC interface. The oscillations manifest themselves in the oscillating dependence of the critical temperature on the AFM thickness.

The predicted oscillating behavior of the critical temperature is qualitatively similar to the oscillations observed in a number of experimental studies of the critical temperature of AFM/SC bilayers [46–48] and can provide a plausible explanation of these experimental findings. A quantitative comparison between the presented theory and experimental results is difficult because our model does not take into account influence of impurities and finite interface barrier. At the same time it is known that nonmagnetic impurities can provide additional suppression of superconductivity [43] and, therefore, should also contribute to the experimental results. Nevertheless, our results demonstrate that the oscillating behavior of the critical temperature in AFM/SC bilayers can be a signature of the presence of proximity-induced Néel-type triplet correlations in the antiferromagnet.

ACKNOWLEDGMENT

The financial support from the Russian Science Foundation via the RSF project No. 22-22-00522 is acknowledged.

APPENDIX: CALCULATION OF THE NORMAL-STATE GREEN'S FUNCTION

Let us define the following expansion of a Green's function in the basis of Pauli matrices in sublattice space:

$$\check{g}_\sigma = \sum_i \check{g}_{\sigma,i}\rho_i, \quad i \in \{0, x, y, z\}. \tag{A1}$$

Then in the normal state, Eq. (2) takes the form

$$\begin{aligned} \pm iv\frac{d}{dx}\check{g}^{\pm}_{N,0} &= 0, \\ 2h(x)\sigma\check{g}^{\pm}_{N,z} \pm iv\frac{d}{dx}\check{g}^{\pm}_{N,x} &= 0, \\ 2[\omega_m - i\mu(x)]\check{g}^{\pm}_{N,z} \pm iv\frac{d}{dx}\check{g}^{\pm}_{N,y} &= 0, \\ -2\sigma h(x)\check{g}^{\pm}_{N,x} - 2[\omega_m - i\mu(x)]\check{g}^{\pm}_{N,y} & \\ \pm iv\frac{d}{dx}\check{g}^{\pm}_{N,z} &= 0. \end{aligned} \tag{A2}$$

Here $h(x) = h\Theta(-x)$ and $\mu(x) = \mu_{\rm AFM}\Theta(-x) + \mu_{\rm SC}\Theta(x)$. Expanding normalization condition (3) over the Pauli matrices we obtain

$$\check{g}_{N,0}(x) = 0, \quad \check{g}_{N,x}(x)^2 + \check{g}_{N,y}(x)^2 + \check{g}_{N,z}(x)^2 = 1. \tag{A3}$$

In the SC region the solution of Eq. (A2) accounting for the normalization condition takes the form

$$\begin{aligned} \check{g}^{\rm SC}_{N,x}(x) &= G, \\ \check{g}^{\rm SC}_{N,y}(x) &= iDe^{\lambda x} - iEe^{-\lambda x}, \\ \check{g}^{\rm SC}_{N,z}(x) &= De^{\lambda x} + Ee^{-\lambda x}. \end{aligned} \tag{A4}$$

In the AFM region the solution takes the form

$$\begin{aligned} \check{g}^{\rm AFM}_{N,x}(x) &= A + \frac{ih\sigma B}{\Lambda}e^{\beta x} + \frac{-ih\sigma C}{\Lambda}e^{-\beta x}, \\ \check{g}^{\rm AFM}_{N,y}(x) &= A\frac{h\sigma}{i(\mu_{\rm AFM} + i\omega_m)} + \frac{(\mu_{\rm AFM} + i\omega_m)B}{\Lambda}e^{\beta x} \\ &\quad + \frac{-(\mu_{\rm AFM} + i\omega_m)C}{\Lambda}e^{-\beta x}, \\ \check{g}^{\rm AFM}_{N,z}(x) &= Be^{\beta x} + Ce^{-\beta x}, \end{aligned} \tag{A5}$$

where $\lambda = 2(\omega_m - i\mu_{\rm SC})/v$, $\beta = 2\Lambda/v$, $\Lambda = [h^2 - (\mu_{\rm AFM} + i\omega_m)^2]^{1/2}$, A, B, C, D, E, and G are unknown coefficients. Equation (3) takes the form

$$4BC + A^2\left(1 - \frac{h^2}{(\mu_{\rm AFM} + i\omega_m)^2}\right) = 1, \quad 4DE + G^2 = 1. \tag{A6}$$

To find the coefficients A, B, C, D, E, and G, we should take into account two trajectories with $v_{F,x} = \pm v$. Boundary conditions at $x = +d_{\rm SC}$, $x = -d_{\rm AFM}$, and $x = 0$ take the form

$$\check{g}_N^{\rm SC,+}(x = +d_{\rm SC}) = \check{g}_N^{\rm SC,-}(x = +d_{\rm SC}),$$
$$\check{g}_N^{\rm AFM,+}(x = -d_{\rm AFM}) = \check{g}_N^{\rm AFM,-}(x = -d_{\rm AFM}),$$
$$\check{g}_N^{\rm SC,\pm}(x = 0) = \check{g}_N^{\rm AFM,\pm}(x = 0). \tag{A7}$$

Substituting Eqs. (A4) and (A5) into Eq. (A7) we obtain

$$B = \frac{h\sigma}{2\sqrt{B_0}}, \text{ with} \tag{A8}$$

$$B_0 = \left(\mu_{\rm AFM}^2 - h^2\right)\cosh^2(\beta d_{\rm AFM}) + i\mu_{\rm AFM}\sqrt{h^2 - \mu_{\rm AFM}^2}\sinh(2\beta d_{\rm AFM})\coth(\lambda d_{\rm SC}) + \left[\mu_{\rm AFM}^2\coth^2(\lambda d_{\rm SC}) - h^2\sinh^{-2}(\lambda d_{\rm SC})\right]\sinh(\beta d_{\rm AFM}), \tag{A9}$$

$$C = -B, \quad D = -B\frac{\sinh(\beta d_{\rm AFM})}{\sinh(\lambda d_{\rm SC})}, \quad E = -D, \tag{A10}$$

$$A = \frac{B}{h\sigma}\left\{[-1 + \coth(\lambda d_{\rm SC})]\left(\cosh(\lambda d_{\rm SC})\sinh(\beta d_{\rm AFM}) - \frac{i\mu_{\rm AFM}\cosh(\beta d_{\rm AFM})\sinh(\lambda d_{\rm SC})}{\sqrt{h^2 - \mu_{\rm AFM}^2}}\right)2e^{\lambda d_{\rm SC}}\mu_{\rm AFM}\right\}, \tag{A11}$$

$$G = \frac{2B}{h\sigma}\left(\sqrt{h^2 - \mu_{\rm AFM}^2}\cosh(\beta d_{\rm AFM}) + \mu_{\rm AFM}\coth(\lambda d_{\rm SC})\sinh(\beta d_{\rm AFM})\right). \tag{A12}$$

In case of $\mu_{\rm SC} = 0$ (it is the case under consideration) solution for coefficients for anomalous Green's function $L_{1,\sigma}^{\pm}, L_{2,\sigma}^{\pm}$ can be simplified and written here (the full solution can be also obtained, but it is rather long),

$$L_{1,\sigma}^{\pm} - L_{2,\sigma}^{\pm} = 2\frac{X\cosh(\hat{\nu}_1^{\pm}) - Y^{\pm}\frac{h\sigma\mu_{\rm AFM}}{\mu_{\rm AFM}^2 - h^2}\coth^2(\hat{\kappa}_1^{\pm})\sinh(\hat{\nu}_1^{\pm}) - \left[Y^{\pm}h\sigma\cosh(\hat{\nu}_1^{\pm}) - X\mu_{\rm AFM}\sinh(\hat{\nu}_1^{\pm})\right]\frac{\coth(\hat{\kappa}_1^{\pm})}{\sqrt{\mu_{\rm AFM}^2 - h^2}}}{\left[\cosh(\hat{\nu}_1^{\pm}) + \frac{\mu_{\rm AFM}}{\sqrt{\mu_{\rm AFM}^2 - h^2}}\coth(\hat{\kappa}_1^{\pm})\sinh(\hat{\nu}_1^{\pm})\right]^2}, \tag{A13}$$

where

$$\hat{\nu}_1^{\pm} = \frac{\mp i\nu_1 d_{\rm SC}}{v}, \quad \hat{\kappa}_1^{\pm} = \frac{\mp i\kappa_1 d_{\rm AFM}}{v}, \quad X = -\frac{(\hat{G}_\sigma^{\pm}\hat{s}_1)}{\nu_1|s_1|^2}, \quad Y^{\pm} = -\frac{\mp i d_{\rm SC}}{v}\frac{(\hat{G}_\sigma^{\pm}\hat{s}_4)}{|s_4|^2}. \tag{A14}$$

[1] A. I. Buzdin, Proximity effects in superconductor-ferromagnet heterostructures, Rev. Mod. Phys. **77**, 935 (2005).

[2] F. S. Bergeret, A. F. Volkov, and K. B. Efetov, Odd triplet superconductivity and related phenomena in superconductor-ferromagnet structures, Rev. Mod. Phys. **77**, 1321 (2005).

[3] M. Eschrig, Spin-polarized supercurrents for spintronics: A review of current progress, Rep. Prog. Phys. **78**, 104501 (2015).

[4] J. Linder and J. W. A. Robinson, Superconducting spintronics, Nat. Phys. **11**, 307 (2015).

[5] A. I. Buzdin, L. N. Bulaevskii, and S. V. Panyukov, Critical-current oscillations as a function of the exchange field and thickness of the ferromagnetic metal (*F*) in an *S-F-S* Josephson junction, Pis'ma Zh. Eksp. Teor. Fiz. **35**, 147 (1982) [JETP Lett. **35**, 178 (1982)].

[6] E. A. Demler, G. B. Arnold, and M. R. Beasley, Superconducting proximity effects in magnetic metals, Phys. Rev. B **55**, 15174 (1997).

[7] A. I. Larkin and Y. N. Ovchinnikov, Nonuniform state of superconductors, Zh. Eksp. Teor. Fiz. **47**, 1136 (1964) [Sov. Phys. JETP **20**, 762 (1965)].

[8] P. Fulde and R. A. Ferrell, Superconductivity in a strong spin-exchange field, Phys. Rev. **135**, A550 (1964).

[9] T. Kontos, M. Aprili, J. Lesueur, F. Genêt, B. Stephanidis, and R. Boursier, Josephson junction through a thin ferromagnetic layer: Negative coupling, Phys. Rev. Lett. **89**, 137007 (2002).

[10] V. V. Ryazanov, V. A. Oboznov, A. Y. Rusanov, A. V. Veretennikov, A. A. Golubov, and J. Aarts, Coupling of two superconductors through a ferromagnet: Evidence for a π junction, Phys. Rev. Lett. **86**, 2427 (2001).

[11] V. A. Oboznov, V. V. Bol'ginov, A. K. Feofanov, V. V. Ryazanov, and A. I. Buzdin, Thickness dependence of the Josephson ground states of superconductor-ferromagnet-superconductor junctions, Phys. Rev. Lett. **96**, 197003 (2006).

[12] A. A. Bannykh, J. Pfeiffer, V. S. Stolyarov, I. E. Batov, V. V. Ryazanov, and M. Weides, Josephson tunnel junctions with

a strong ferromagnetic interlayer, Phys. Rev. B **79**, 054501 (2009).
[13] J. W. A. Robinson, S. Piano, G. Burnell, C. Bell, and M. G. Blamire, Critical current oscillations in strong ferromagnetic π junctions, Phys. Rev. Lett. **97**, 177003 (2006).
[14] T. Yamashita, K. Tanikawa, S. Takahashi, and S. Maekawa, Superconducting π qubit with a ferromagnetic Josephson junction, Phys. Rev. Lett. **95**, 097001 (2005).
[15] A. K. Feofanov, V. A. Oboznov, V. V. Bol'ginov, J. Lisenfeld, S. Poletto, V. V. Ryazanov, A. N. Rossolenko, M. Khabipov, D. Balashov, A. B. Zorin, P. N. Dmitriev, V. P. Koshelets, and A. V. Ustinov, Implementation of superconductor/ferromagnet/superconductor π-shifters in superconducting digital and quantum circuits, Nat. Phys. **6**, 593 (2010).
[16] A. V. Shcherbakova, K. G. Fedorov, K. V. Shulga, V. V. Ryazanov, V. V. Bolginov, V. A. Oboznov, S. V. Egorov, V. O. Shkolnikov, M. J. Wolf, D. Beckmann, and A. V. Ustinov, Fabrication and measurements of hybrid Nb/Al Josephson junctions and flux qubits with π-shifters, Supercond. Sci. Technol. **28**, 025009 (2015).
[17] Y. V. Fominov, N. M. Chtchelkatchev, and A. A. Golubov, Nonmonotonic critical temperature in superconductor/ferromagnet bilayers, Phys. Rev. B **66**, 014507 (2002).
[18] Z. Radović, M. Ledvij, L. Dobrosavljević-Grujić, A. I. Buzdin, and J. R. Clem, Transition temperatures of superconductor-ferromagnet superlattices, Phys. Rev. B **44**, 759 (1991).
[19] B. P. Vodopyanov and L. R. Tagirov, Oscillations of superconducting transition temperature in strong ferromagnet-superconductor bilayers, JETP Lett. **78**, 555 (2003).
[20] L. Lazar, K. Westerholt, H. Zabel, L. R. Tagirov, Y. V. Goryunov, N. N. Garif'yanov, and I. A. Garifullin, Superconductor/ferromagnet proximity effect in Fe/Pb/Fe trilayers, Phys. Rev. B **61**, 3711 (2000).
[21] A. Buzdin, Density of states oscillations in a ferromagnetic metal in contact with a superconductor, Phys. Rev. B **62**, 11377 (2000).
[22] M. Zareyan, W. Belzig, and Y. V. Nazarov, Oscillations of Andreev states in clean ferromagnetic films, Phys. Rev. Lett. **86**, 308 (2001).
[23] J. S. Jiang, D. Davidović, D. H. Reich, and C. L. Chien, Oscillatory superconducting transition temperature in Nb/Gd multilayers, Phys. Rev. Lett. **74**, 314 (1995).
[24] L. V. Mercaldo, C. Attanasio, C. Coccorese, L. Maritato, S. L. Prischepa, and M. Salvato, Superconducting-critical-temperature oscillations in Nb/CuMn multilayers, Phys. Rev. B **53**, 14040 (1996).
[25] T. Mühge, N. N. Garif'yanov, Y. V. Goryunov, G. G. Khaliullin, L. R. Tagirov, K. Westerholt, I. A. Garifullin, and H. Zabel, Possible origin for oscillatory superconducting transition temperature in superconductor/ferromagnet multilayers, Phys. Rev. Lett. **77**, 1857 (1996).
[26] V. Zdravkov, A. Sidorenko, G. Obermeier, S. Gsell, M. Schreck, C. Müller, S. Horn, R. Tidecks, and L. R. Tagirov, Reentrant superconductivity in $Nb/Cu_{1-x}Ni_x$ bilayers, Phys. Rev. Lett. **97**, 057004 (2006).
[27] V. I. Zdravkov, J. Kehrle, G. Obermeier, S. Gsell, M. Schreck, C. Müller, H.-A. Krug von Nidda, J. Lindner, J. Moosburger-Will, E. Nold, R. Morari, V. V. Ryazanov, A. S. Sidorenko, S. Horn, R. Tidecks, and L. R. Tagirov, Reentrant superconductivity in superconductor/ferromagnetic-alloy bilayers, Phys. Rev. B **82**, 054517 (2010).
[28] V. Baltz, A. Manchon, M. Tsoi, T. Moriyama, T. Ono, and Y. Tserkovnyak, Antiferromagnetic spintronics, Rev. Mod. Phys. **90**, 015005 (2018).
[29] T. Jungwirth, X. Marti, P. Wadley, and J. Wunderlich, Antiferromagnetic spintronics, Nat. Nanotechnol. **11**, 231 (2016).
[30] A. Brataas, B. van Wees, O. Klein, G. de Loubens, and M. Viret, Spin insulatronics, Phys. Rep. **885**, 1 (2020).
[31] B. M. Andersen, I. V. Bobkova, P. J. Hirschfeld, and Y. S. Barash, $0-\pi$ transitions in josephson junctions with antiferromagnetic interlayers, Phys. Rev. Lett. **96**, 117005 (2006).
[32] H. Enoksen, J. Linder, and A. Sudbø, Pressure-induced 0-π transitions and supercurrent crossover in antiferromagnetic weak links, Phys. Rev. B **88**, 214512 (2013).
[33] I. V. Bobkova, P. J. Hirschfeld, and Y. S. Barash, Spin-dependent quasiparticle reflection and bound states at interfaces with itinerant antiferromagnets, Phys. Rev. Lett. **94**, 037005 (2005).
[34] B. M. Andersen, I. V. Bobkova, P. J. Hirschfeld, and Y. S. Barash, Bound states at the interface between antiferromagnets and superconductors, Phys. Rev. B **72**, 184510 (2005).
[35] L. G. Johnsen, S. H. Jacobsen, and J. Linder, Magnetic control of superconducting heterostructures using compensated antiferromagnets, Phys. Rev. B **103**, L060505 (2021).
[36] G. A. Bobkov, I. V. Bobkova, A. M. Bobkov, and A. Kamra, Néel proximity effect at antiferromagnet/superconductor interfaces, Phys. Rev. B **106**, 144512 (2022).
[37] G. A. Bobkov, I. V. Bobkova, and A. M. Bobkov, Proximity effect in superconductor/antiferromagnet hybrids: Néel triplets and impurity suppression of superconductivity, Phys. Rev. B **108**, 054510 (2023).
[38] S. Chourasia, L. J. Kamra, I. V. Bobkova, and A. Kamra, Generation of spin-triplet Cooper pairs via a canted antiferromagnet, Phys. Rev. B **108**, 064515 (2023).
[39] D. S. Rabinovich, I. V. Bobkova, and A. M. Bobkov, Anomalous phase shift in a Josephson junction via an antiferromagnetic interlayer, Phys. Rev. Res. **1**, 033095 (2019).
[40] V. Falch and J. Linder, Giant magnetoanisotropy in the Josephson effect and switching of staggered order in antiferromagnets, Phys. Rev. B **106**, 214511 (2022).
[41] M. F. Jakobsen, K. B. Naess, P. Dutta, A. Brataas, and A. Qaiumzadeh, Electrical and thermal transport in antiferromagnet-superconductor junctions, Phys. Rev. B **102**, 140504(R) (2020).
[42] J. L. Lado and M. Sigrist, Two-dimensional topological superconductivity with antiferromagnetic insulators, Phys. Rev. Lett. **121**, 037002 (2018).
[43] E. H. Fyhn, A. Brataas, A. Qaiumzadeh, and J. Linder, Superconducting proximity effect and long-ranged triplets in dirty metallic antiferromagnets, Phys. Rev. Lett. **131**, 076001 (2023).
[44] G. A. Bobkov, I. V. Bobkova, and A. A. Golubov, Magnetic anisotropy of the superconducting transition in superconductor/antiferromagnet heterostructures with spin-orbit coupling, Phys. Rev. B **108**, L060507 (2023).
[45] L. Johnsen Kamra, S. Chourasia, G. A. Bobkov, V. M. Gordeeva, I. V. Bobkova, and A. Kamra, Infinite magnetoresistance and Néel triplets-mediated exchange in

antiferromagnet-superconductor-antiferromagnet trilayers, Phys. Rev. B **108**, 144506 (2023).

[46] C. Bell, E. J. Tarte, G. Burnell, C. W. Leung, D.-J. Kang, and M. G. Blamire, Proximity and Josephson effects in superconductor/antiferromagnetic $Nb/\gamma - Fe_{50}Mn_{50}$ heterostructures, Phys. Rev. B **68**, 144517 (2003).

[47] M. Hübener, D. Tikhonov, I. A. Garifullin, K. Westerholt, and H. Zabel, The antiferromagnet/superconductor proximity effect in Cr/V/Cr trilayers, J. Phys.: Condens. Matter **14**, 8687 (2002).

[48] B. L. Wu, Y. M. Yang, Z. B. Guo, Y. H. Wu, and J. J. Qiu, Suppression of superconductivity in Nb by IrMn in IrMn/Nb bilayers, Appl. Phys. Lett. **103**, 152602 (2013).

[49] A. Zaitsev, Quasiclassical equations of the theory of superconductivity for contiguous metals and the properties of constricted microcontacts, Zh. Eksp. Teor. Fiz. **86**, 1742 (1984) [Sov. Phys. JETP **59**, 1015 1984].

[50] A. Millis, D. Rainer, and J. A. Sauls, Quasiclassical theory of superconductivity near magnetically active interfaces, Phys. Rev. B **38**, 4504 (1988).